

Designing and Simulation of 30Gbps FSO Communication Link Under Different Atmospheric and Cloud Conditions

Pranav Bhatt¹, Dr.Bhavin Sedani², Dr.Nirali Kotak³

¹Research Scholar, Electronics and Communication Department, L.D. College of Engineering-Ahmedabad, Gujarat Technological University, Gujarat, India.

²Professor, Electronics and Communication Department, L.D. College of Engineering-Ahmedabad, Gujarat Technological University, Gujarat, India.

³Assistant Professor, Electronics and Communication Department, L.D. College of Engineering-Ahmedabad, Gujarat Technological University, Gujarat, India.

¹pranavm153@gmail.com, ²bhavin_s_sedani@yahoo.com, ³nakotak@ldce.ac.in

Abstract — RF communication has inherent limitations in terms of bandwidth (data capacity). Upcoming satellite technology demands a higher data rate and higher reliability, i.e., a lower bit error rate. Now Free-space optical communication (FSO) is basically an emerging optical wireless communication technique, which can provide extremely high data rates because it operates on frequencies above 300 GHz. This paper simulates 30 Gbps ground-to-geostationary satellite-FSO communication link under different atmospheric effects like haze & fog; and under different types of cloud-like stratus, cumulus & cumulonimbus; while doing so, the effect of moderate atmospheric turbulence and intensity scintillation is always considered. The work shows that a 2×2 MIMO system having QPSK modulation with coherent detection and digital signal processing gives an extremely low symbol error rate in almost all weather and all cloud conditions.

Keywords — FSO link, Atmospheric Turbulence, Intensity Scintillation, SER.

I. INTRODUCTION

For more than a half-century, RF communication successfully meets our demands in terms of data rates and channel reliability for satellite communication [24]. However, RF is inherently limited in terms of bandwidth (data capacity) and cost (licensing fees). The highest data rate ever achieved for Ground-to-Geostationary satellite link using RF communication at Ka-band (26.5–40 GHz) is 2 Gbps (for 16 Amplitude-phase shift keying modulation) with a bit error rate (BER) of 10^{-9} [10]. However, in the laboratory, the demonstrated data rates were 5.7 Gbps (for Quadrature Phase Shift Keying modulation) and 20 Gbps (for 128-Quadratur amplitude modulation) with a BER of 10^{-9} [10]. The improved alternative for RF communication is Free-space optical communication (FSO). FSO or Optical wireless communication (OWC) link is a wireless communication link that uses optically modulated data transmitted through an unguided medium like atmosphere [1]. The FSO channels operate on frequencies of more than

300GHz; thus, they can offer colossal bandwidth and extremely high data rates [2].

FSO communication framework comprises three sections; transmitter, atmospheric channel, and receiver. In the transmitter part, initially, some modulation scheme modulates the input information. After that, the optical modulator and the optical source (laser diode) transforms the modulated signal into an optical signal. As the optical signal passes through the atmospheric channel, it is attenuated due to atmospheric turbulence, scattering, and absorption [4]. The atmospheric attenuation due to fog, haze, rainfall, and scintillation causes significant degradation of the signal [25]. At the receiver part, the optical signal is cumulated using a telescope lens, converted into an electrical signal, and demodulated. The majority of FSO systems are designed to operate in the atmospheric windows of 780–850nm and 1520–1600nm because of lower atmospheric absorption and availability of readily designed fiber optics hardware in this range [3]. Besides, FSO communications are LOS communications, providing us with a direct advantage of security. The binary phase-shift keying (BPSK) is the most widely recognized modulation scheme in the field of satellite communication. Here in this work, 30Gbps Ground-to-Geostationary Satellite-FSO communication link under different atmospheric effects and different cloud conditions in the presence of turbulence and scintillation is simulated using QPSK modulation technique with coherent detection and digital signal processing in addition to spatial diversity. The reason behind the selection of QPSK modulation is its half bandwidth compared to BPSK, doubled data rate compared to BPSK, and the better BER performance than all other PSK techniques [5]. For spatial diversity, multiple optical transmitters and multiple optical receivers are used to decrease the atmosphere's effect with the help of different spatial paths. The data rates achieved in this work are around three times higher than demonstrated data rate for RF Ka-band communication for the same modulation scheme [10]. This paper is arranged as follows. Section II explains the internal architecture of the Optical QPSK transmitter and Optical coherent QPSK



receiver. Section III describes the importance of DSP in simulated work. In section IV, the design architecture of 2x2 MIMO is shown. Section V calculates the values of OWC parameters like attenuation for different weather and cloud condition. Section VI and VII are for simulation setup and simulation results. Section VIII compares the proposed work with previous work, and section IX stands for the conclusion. Both the words, Free-Space Optical (FSO) communication and Optical Wireless Communication (OWC), are used interchangeably in this work.

II. SYSTEM ARCHITECTURE

Fig. 1 portrays the Optical QPSK transmitter architecture. A pseudo-random bit sequence (PRBS) generator roughly simulates the behavior of random binary data. PSK sequence generator produces two parallel M-ary symbol sequences. These M-ary symbols are transformed to multi-level pulses using an M-ary pulse generator. For QPSK, each M-ary pulse generator produces the pulses that are of 2 levels. After that, the Mach-Zehnder modulator is used for optical modulation, which encodes QPSK pulses on an optical carrier signal. The branch with a 90° phase shifter represents the quadrature-phase component (Q), and the other one represents the in-phase component (I). The last process is to couple both I and Q components using a cross coupler.

In optical coherent QPSK receiver, as shown in Fig. 2, outputs of 2x4 90° hybrid are given to balanced photodetectors. The hybrid's inputs are received optical signal from the OWC channel and continuous wave (CW) laser (as a local oscillator). The hybrid has four 3 dB couplers and a 90° phase shifter in the lower branch, which together lets the receiver extract the in-phase (I) and quadrature-phase (Q) signal components [7]. The electrical

I and Q outputs from balanced detectors are given to DSP. DSP performs necessary signal processing operations, which are discussed in sub-section c. The threshold detection/decision converts processed I and Q signals to M-ary symbols, which are then given to the PSK sequence decoder. For an ideal lossless system, the PSK sequence decoder's output should be the input binary pseudo-random bit sequence.

III. IMPORTANCE OF QPSK-DSP

The DSP is the most crucial part of this system. It is used after coherent reception of the signal to overcome channel impairments caused by the atmosphere [21]. The design of the proposed DSP is in Fig. 3. The Bessel filter provides linear phase response, which is essential for phase shift keying techniques; it also removes the band noise [22]. The chromatic dispersion due to atmosphere and inter-symbol interference is compensated with the help of an adaptive equalizer [23]. The adaptive equalizer works by using the constant modulus algorithm [23]. Finally, the carrier phase estimator removes the symbol spread occurring due to the linewidth of laser and phase mismatch occurring due to coherent detection using a blind phase search algorithm.

IV. 2x2 MIMO

For the Ground-to-Geostationary satellite communication link, the beam divergence of the transmitted optical beam needs to be extremely small; otherwise, the receiver aperture size will not be practically feasible. When using spatial diversity, due to the beam's narrowness and the small separation between transmitting sources, the channel losses are almost identical in both spatial paths (as in the case of 2x2 MIMO).

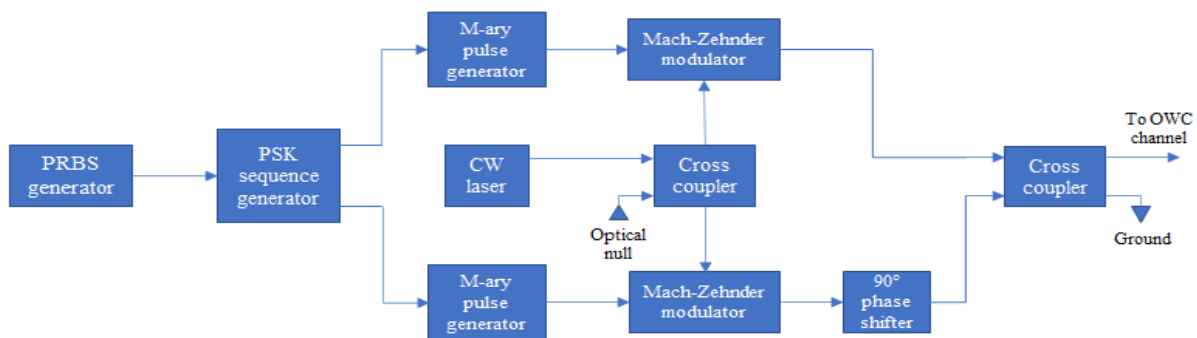


Fig. 1 Optical QPSK transmitter

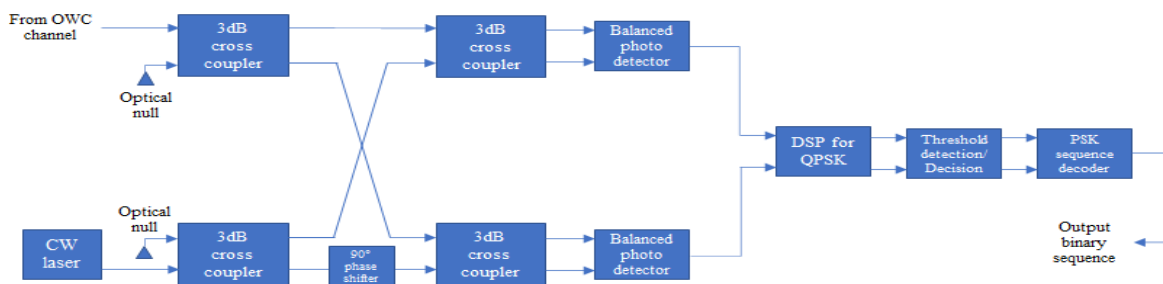


Fig. 2 Optical coherent QPSK receiver with post-processing



Fig 3. Proposed DSP block diagram

V. OPTICAL WIRELESS CHANNEL PARAMETERS

The atmosphere is highly random in nature. The optical signal passing through the atmosphere are largely affected by atmospheric turbulence and atmospheric attenuation. As indicated by the Kruse formula, the atmospheric attenuation coefficient (α) is determined with the help of the visibility and the wavelength of the optical beam. Because of its precision Kruse formula is widely used for the calculation of atmospheric attenuation [8].

$$\alpha = \frac{3.91}{V} \left(\frac{\lambda}{\lambda_0} \right)^{-q} \tag{1}$$

In (1), λ is the wavelength of the optical beam (nm), V is visibility (Km), λ_0 is reference wavelength (550 nm), and q is scattering particle size distribution. According to the Kruse model for $V > 50$ Km, the value q is 1.6, for $6 \text{ Km} < V < 50 \text{ Km}$ it is 1.3, and for $V < 6 \text{ Km}$, q it is measured using (2).

$$q = 0.585V^{\frac{1}{3}} + 0.34 \tag{2}$$

Here, in this work, 1550 nm is used as a wavelength of the optical transmitted optical beam. According to that, Table I and Table III contains visibility values, and Table II and Table IV contain attenuation values calculated at 1550nm wavelength using respective visibility values.

TABLE I
VISIBILITY VALUE FOR DIFFERENT WEATHER CONDITIONS [9]

Weather condition	Visibility (Km)
Clear air	94
Haze	2
Light fog	0.8
Moderate fog	0.6
Heavy fog	0.05

TABLE II
ATMOSPHERIC ATTENUATION FOR DIFFERENT WEATHER CONDITIONS AT 1550NM WAVELENGTH

Weather condition	Attenuation (dB/Km)
Clear air	0.008
Haze	0.645
Light fog	1.964
Moderate fog	2.758
Heavy fog	43.77

TABLE III
VISIBILITY VALUE FOR DIFFERENT TYPES CLOUD [8]

Cloud type	Visibility (Km)
Stratus	29.14
Cumulus	27.82
Cumulonimbus	65
Stratocumulus	38.75
Cirrus	7.13

TABLE IV
ATTENUATION DUE TO DIFFERENT TYPES OF CLOUDS AT 1550NM WAVELENGTH

Cloud type	Attenuation (dB/Km)
Stratus	0.035
Cumulus	0.037
Cumulonimbus	0.011
Stratocumulus	0.026
Cirrus	0.143

The Refractive index structure parameter $C_n^2 (m^{-\frac{2}{3}})$ is the most important parameter that governs the behavior of turbulence [10]. For long distances, we can suppose it to be practically constant. For moderate turbulence, the refractive index structure parameter is around $10^{-15} m^{-\frac{2}{3}}$ [11]. The effect of intensity scintillation is modeled using the gamma-gamma turbulence model, which represents atmospheric fading [12]. The Probability of intensity is calculated using small scale eddy variance, large scale eddy variance, Gamma function, and second

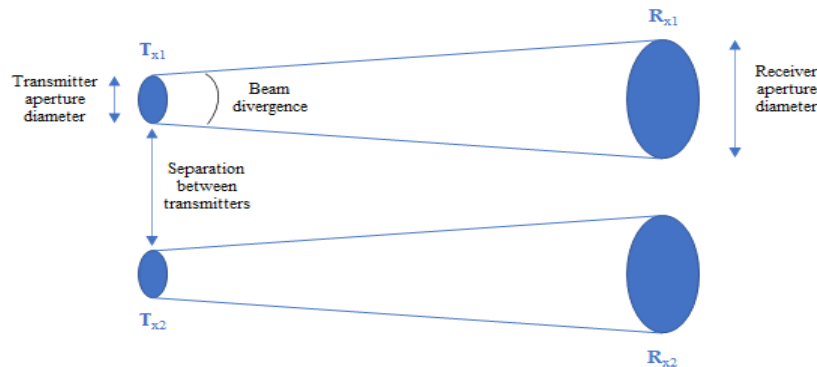


Fig. 4 2x2 MIMO-FSO

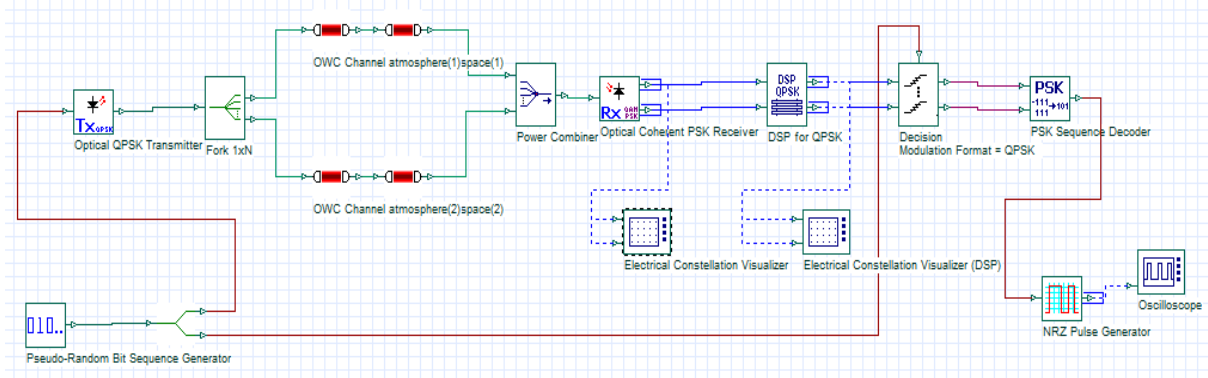


Fig. 5 Optisystem-17 simulation setup

Kind modified Bessel function. Small scale eddy variance and large scale eddy variance are calculated using Rytov variance, and Rytov variance itself is calculated using refractive index structure parameter, optical wavenumber (m^{-1}) of the signal, and range [13]. Here (3), (4), (5), and (6) show a complex relationship between turbulence and intensity scintillation.

$$\sigma_R^2 = 1.23 C_n^2 k^{\frac{7}{6}} z^{\frac{11}{6}} \quad (3)$$

$$P(I) = \frac{2(\alpha\beta)^{\frac{(\alpha+\beta)}{2}}}{\Gamma(\alpha)\Gamma(\beta)} \cdot I^{\frac{(\alpha+\beta)}{2-1}} \cdot K_{\alpha-\beta}(2\sqrt{\alpha\beta}I) \quad (4)$$

$$\alpha = \exp\left[\frac{0.49\sigma_R^2}{(1 + 1.11\sigma_R^{\frac{12}{5}})^{\frac{5}{6}}}\right] - 1 \quad (5)$$

$$\beta = \exp\left[\frac{0.51\sigma_R^2}{(1 + 0.69\sigma_R^{\frac{12}{5}})^{\frac{5}{6}}}\right] - 1 \quad (6)$$

In (3), (4), (5), and (6) σ_R^2 is Rytov variance, C_n^2 is refractive index structure parameter ($m^{-\frac{2}{3}}$), k is optical wavenumber (m^{-1}), z is range (Km), $\frac{1}{\alpha}$ is small scale eddy variance, $\frac{1}{\beta}$ is large scale eddy variance, $\Gamma(\alpha), \Gamma(\beta)$ are Gamma functions, $K_{\alpha-\beta}(2\sqrt{\alpha\beta}I)$ is the second kind

modified Bessel function and $P(I)$ is the probability of intensity.

VI. SIMULATION SETUP

Design and simulation of the proposed framework are done utilizing optisystem-17, as displayed in Fig. 5. Optisystem-17 can configuration, test, and simulate almost all modern optical systems.

1550 nm is selected as the emission wavelength for the Optical QPSK transmitter. The reasons for selecting this particular wavelength are the availability of atmospheric windows (1520-1600 nm) [3], low molecular absorption, and eye safety [14].

The optical QPSK transmitter is connected to a fork, the function of which is to create identical copies of the signals, so always the value of outgoing signal/signals is equal to the value of the incoming signal. At the receiver, the power arriving from the two channels is merged by a power combiner and then given to the optical coherent PSK receiver. Fork and power combiner together creates a 2x2 MIMO system, as shown in Fig. 4. The constellation visualizer is used to show I and Q signals in a constellation diagram. It also calculates symbol error rate and Q-factor with the help of error vector magnitude and symbol error estimation.

To create one ground-to-geostationary satellite channel, two OWC channels are connected serially, as shown in Fig. 5. OWC channel that represents atmosphere is of 12 Km length. This particular

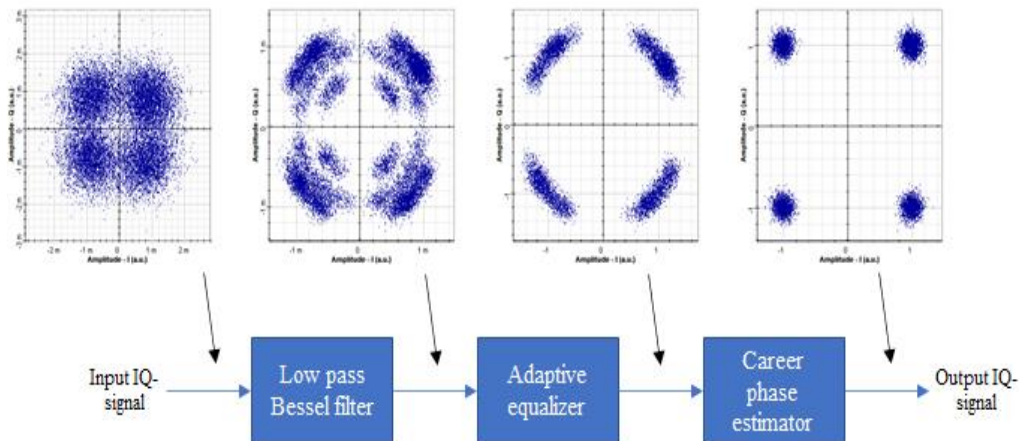


Fig. 6 Constellation diagram at different stages of QPSK-DSP

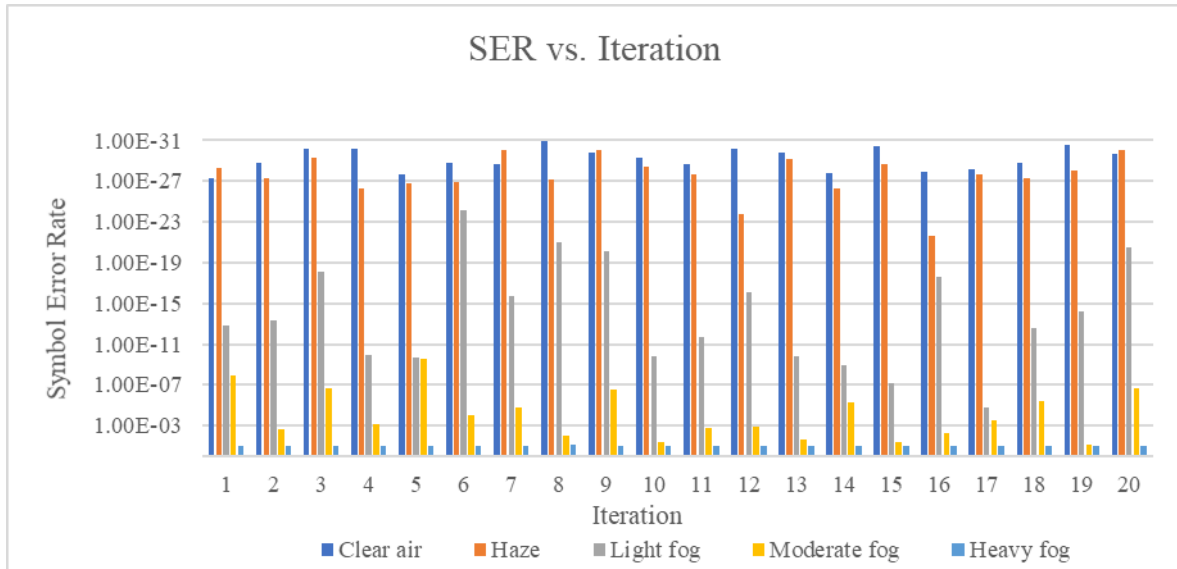


Fig. 7 Symbol Error Rate vs. Iteration for different weather conditions [simulation values from Table II]

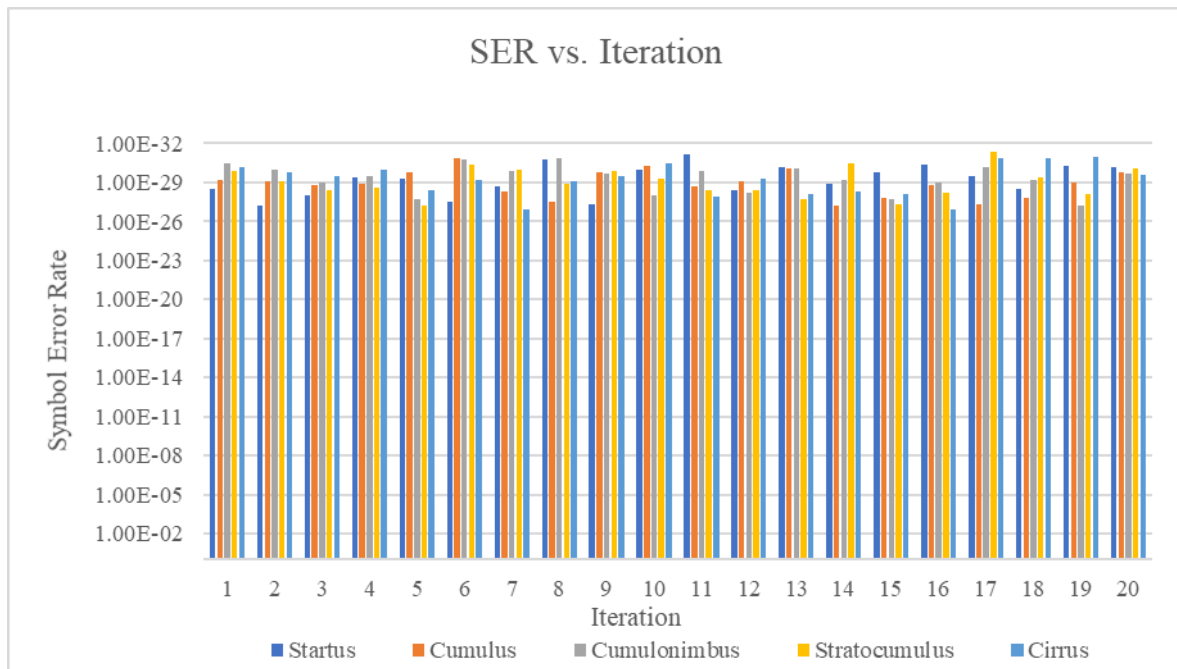


Fig. 8 Symbol Error Rate vs. Iteration for different types of clouds [simulation values Table IV]

Length for the atmospheric channel is selected by averaging the elevation of the tropopause because at the pole, the tropopause is at 9 Km from the surface, and at the equator, the tropopause is at 15 km from the surface [15]. The tropopause is the border between the troposphere and stratosphere. The troposphere contains 75% of the atmosphere's mass and 99% of the entire mass of water vapor and aerosols combined [16]. OWC channel representing atmosphere simulates attenuation caused by clear air, haze, different types of fog, and different clouds. It also simulates moderate atmospheric turbulence and scintillation. Another OWC channel represents a space channel, which has 35,988 Km length. It is just used for geometric loss, which is a fixed value because it depends on beam divergence and transmitter-receiver aperture diameter only. Simulation is iterated 20 times in series for

each weather condition and each cloud type to consider the effect of atmospheric turbulence and scintillation.

TABLE V
SIMULATION PARAMETERS

Parameter	Value
Emission wavelength	1550 nm
Bit rate	30 Gbps
Link distance	36000 Km (GND-GEO)
Sequence length	16384 bits
Samples/bit	32
Modulation technique	QPSK
Transmitter power	10 dBm
Coherent receiver power	10 dBm
Laser linewidth	0.1 MHz

Refractive index structure parameter	$5 \times 10^{-15} m^{-\frac{2}{3}}$
Geometric loss	10 dB
Number of iterations	20

TABLE VI
DSP SETUP PARAMETERS

Parameter	Value
Bessel filter cutoff frequency	11.25 GHz
Adaptive equalization number of taps	9
Order of Dispersion	2
Adaptive equalization number of iterations	15
Step CMA	10^{-6}
Taps index (Initial)	1
Career phase estimation symbols per block	40

VII. RESULTS

Fig. 6 displays the constellation diagram at each stage of DSP. As it is easily visible that the constellation diagram is too messy initially, but it is getting improved after each stage of DSP processing. Without DSP, the SER of the received signal will always be extremely high (probably near to 0).

TABLE VII
MINIMUM AND MAXIMUM SER FOR DIFFERENT WEATHER CONDITION

Weather condition	Minimum SER	Maximum SER
Clear air	1.18E-31	4.62E-28
Haze	9.30E-31	2.26E-22
Light fog	8.26E-25	1.79E-05
Moderate fog	2.80E-10	6.56E-02
Heavy fog	8.38E-02	8.90E-02

TABLE VIII
MINIMUM AND MAXIMUM SER FOR DIFFERENT TYPES OF CLOUD

Type of cloud	Minimum SER	Maximum SER
Stratus	6.67E-32	6.57E-28
Cumulus	1.33E-31	6.58E-28
Cumulonimbus	1.24E-31	5.81E-28
Stratocumulus	4.68E-32	6.12E-28
Cirrus	1.10E-31	1.24E-27

The symbol error rate (SER) is almost constant and extremely low for clear air and all types of clouds. SER is a little fluctuating for the haze but still very low, but for light fog and moderate fog, it is extremely fluctuating. For heavy fog, SER is almost constant but undesirably high. From the results, it can be understood that the designed system will not have desirable SER for heavy fog and moderate fog; however, it might work with light fog with fluctuating SER.

VIII. COMPARISON WITH PREVIOUS WORK

The comparison with previous work takes data rate, link distance, and transmitted power as comparison parameters, as shown in Table IX.

TABLE IX
COMPARISON WITH PREVIOUS WORK

Sr. no.	Data rate (Gbps)	Link distance (Km)	Transmitted power (dBm)	Reference no.
1	10	4000	0	[17]
2	10	20,000	10	[18]
3	2.5	36,000	5	[5]
4	10	40,000	30	[19]
5	30	36,000	10	Proposed work

VIII. CONCLUSION

The FSO technology provides considerably outstanding performance in terms of data rate and symbol error rate compared to RF for ground-to-geostationary satellite communication. By using coherent detection and DSP, the system can provide exceptional reliability, i.e., extremely low SER, under different weather conditions and cloud conditions while also considering the effect of atmospheric turbulence and intensity scintillation

REFERENCES

- [1] K. Kaur, R. Miglani, and G. S. Gaba, Communication theory review perspective on channel modeling, modulation, and mitigation techniques in free-space optical communication, International Journal of Control Theory and Applications, 9(2016) 4969-4978.
- [2] M. A. Khalighi and M. Uysal, Survey on Free Space Optical Communication: A Communication Theory Perspective, IEEE Communications Surveys & Tutorials, 16(2014) 2231-2258.
- [3] H. Kaushal and G. Kaddoum, Optical Communication in Space: Challenges and Mitigation Techniques, IEEE Communications Surveys & Tutorials, 19(2016) 57-96.
- [4] K. Anbarasi, C. Hemanth, and R.G. Sangeetha, A review on channel models in free-space optical communication systems, Optics & Laser Technology, 97(2017)161-171.
- [5] A. P. Bindushree, A. B Nataraju, T. V. Vijesh, and A. S. Laxmiprasad, Design And Simulation Of QPSK Modulator For Optic Inter Satellite Communication, International Journal of Scientific & Technology Research, 3(2014) 402-408.
- [6] N. Singhal, A. Bansal, D. Agarwal, and A. Kumar, A survey on performance enhancement in FSO through spatial diversity and beamforming, in 2015 International Conference on Soft Computing Techniques and Implementations (ICSCTI), (2015) 159-163.
- [7] D. G. Sequeira, L. G. Cancela and J. L. Rebola, Impact of physical layer impairments on multi-degree CDC ROADM-based optical networks, in 2018 International Conference on Optical Network Design and Modeling (ONDM), (2018) 94-99.
- [8] N. Tabassum, N. Franklin, D. Arora, and S. Kaur, "Performance Analysis of Free Space Optics Link for Different Cloud Conditions," in 2018 4th International Conference on Computing Communication and Automation (ICCCA), (2018)1-5.
- [9] H. Ali, E. Said, and M. Yousef, Effect of Environmental Parameters on the Performance of Optical Wireless Communications, International Journal of Optics, (2019) 1-12.
- [10] P. A. Frederickson, K. L. Davidson, C. R. Zeisse and C. S. Bendall, Estimating the Refractive Index Structure Parameter (Cn2) over the Ocean Using Bulk Methods, Journal of Applied Meteorology, 39(2000) 1770-1783.
- [11] S. Basu, A simple approach for estimating the refractive index structure parameter (Cn2) profile in the atmosphere, Optics Letters, 40(2015) 4130-4133.
- [12] L. C. Andrews, R. L. Phillips, C. Y. Hopen, Laser Beam Scintillation with Applications, SPIE Press Book, 2001.

- [13] Larry C. Andrews, Ronald L. Phillips, Laser Beam Propagation Through Random Media, 2nd ed., SPIE Press Book, 2005.
- [14] J. Mukherjee, W. Wulfken, H. Hartje, F. Steinsiek, M. Perren and S. J. Sweeney, Demonstration of eye-safe (1550 nm) terrestrial laser power beaming at 30 m and subsequent conversion into electrical power using dedicated photovoltaics, in 2013 IEEE 39th Photovoltaic Specialists Conference (PVSC), (2013) 1074-1076.
- [15] D.F. Rex, Ed., Climate of the Free Atmosphere, World Survey of Climatology, New York, USA: Elsevier, 4(1969).
- [16] Troposphere, Concise Encyclopedia of Science & Technology, McGraw-Hill, 1984.
- [17] S. Chaudhary, R. Kapoor and A. Sharma, Empirical Evaluation of 4 QAM and 4 PSK in OFDM-based Inter-Satellite Communication System, Journal of Optical Communications, 40(2017) 143-147.
- [18] S. Chaudhary, A. Sharma, and V. Singh, Optimization of high speed and long haul inter-satellite communication link by incorporating differential phase shift key and orthogonal frequency division multiplexing scheme, Optik - International Journal for Light and Electron Optics, 176(2018) 185-190.
- [19] T. Mehmood and N. Hameed. (2017) Electrical Engineering and Systems Science on arXiv. [Online]. Available: <https://arxiv.org/abs/1711.10864>
- [20] R. Simons. (2011) Demonstration of Multi-Gigabit Per Second Data Rates Through Ka-Band Frequencies on FLC [Online]. Available: <https://federallabs.org/news/demonstration-of-multi-gigabit-per-second-data-rates-through-ka-band-frequencies>
- [21] W. Shieh and I. Djordjevic, OFDM for Optical Communications, W. Shieh, I. Djordjevic, Eds. Academic Press: Elsevier, 2010.
- [22] M. T. Thompson, Intuitive Analog Circuit Design, 2nd ed., M. T. Thompson, Ed., Newnes: Elsevier, 2014.
- [23] D. Godard, Self-Recovering Equalization and Carrier Tracking in Two-Dimensional Data Communication Systems, IEEE Transactions on Communications, 28(1980) 1867-1875.
- [24] S. Hussain, N. Bhadri and Md. S. Hussain, Advancement in wireless communication, International Journal of Electronics and Communication Engineering, 7(2020) 1-4.
- [25] J. Kaur and M. Kaur, Design & Investigation of 8x5Gb/s & 8x10Gb/s WDM-FSO Transmission Systems Under Different Atmospheric Conditions, International Journal of Electronics and Communication Engineering, 4(2017) 6-11.